



## Accepted Manuscript

### Impact of Temperature on the Unconfined Compressive Strength of Lime-Stabilized Aeolian Sands

Akbar Cheshomi, Farnaz Safarzadeh

DOI: 10.22059/GEOPE.2025.390214.648806

Receive Date: 09 February 2025

Revise Date: 07 April 2025

Accept Date: 20 April 2025

## Impact of Temperature on the Unconfined Compressive Strength of Lime-Stabilized Aeolian Sands

Akbar Cheshomi \*, Farnaz Safarzadeh

Department of Engineering Geology, College of Science, University of Tehran, Tehran, Iran

Received: 09 February 2025, Revised: 07 April 2025, Accepted: 20 April 2025

### Abstract

Aeolian sands are widely distributed in the Khuzestan Plain and serve as a common borrow material. Lime (CaO) has long been used to improve soil engineering properties. Given the high temperatures in this region, it is essential to assess the impact of temperature on the unconfined compressive strength ( $q_u$ ) of lime-stabilized aeolian sand. In this study, aeolian sand samples were collected and mixed with 5%, 7%, and 9% lime by weight. The samples were cured for 7, 14, and 21 days and then tested at temperatures of 20°C, 30°C, 50°C, and 70°C. According to the Unified Soil Classification System, the tested sand is poorly graded (SP) with an optimum moisture content of 13.18% and a maximum dry density of 1.688 g/cm<sup>3</sup>. The results showed that  $q_u$  increases with curing time and lime content but decreases with higher test temperatures. SEM images revealed that lime particles fill voids and bond sand grains, enhancing strength. However, as temperature increased from 20°C to 70°C, samples with 5%, 7%, and 9% lime (cured for 21 days) showed  $q_u$  reductions of 56%, 48%, and 52%, respectively. Since the samples were tested in dry conditions, this decline is attributed to differences in the thermal expansion of quartz and lime, as well as the increased kinetic energy and fluid volume. An empirical model was proposed to estimate  $q_u$  under varying conditions.

**Keywords:** Aeolian Sands, Lime Stabilization, Unconfined Compressive Strength ( $Q_u$ ), Thermal Effects, Khuzestan Plain.

### Introduction

Currently, soil improvement methods using additives are widely applied worldwide. These techniques enhance geotechnical parameters of the soil, reduce costs, shorten construction time, and extend the service life of structures. Aeolian sands are characterized by poor grading and uniform particle size distribution. The grain size typically falls within the range of 0.08 to 0.80 mm. These sands exhibit high permeability, ranging from  $3.4 \times 10^{-4}$  to  $2 \times 10^{-1}$  cm/s. The pH value of these sands has been reported to range from 7.5 to 8.9 (Abu Seif, 2013; Khan, 1982). Aeolian sands lack plasticity and are difficult to compact due to their uniform particle size distribution. This results in a low bearing capacity (Arias Trujillo et al., 2020). Studies have shown that aeolian sands are prone to collapse when wet (Mohamedzein et al., 2019) and, in loose and saturated conditions, exhibit liquefaction under cyclic loading (Souza Júnior et al., 2020). The range of solid particle specific gravity ( $G_s$ ) for aeolian sands has been reported between 2.44 and 2.87 (Khan, 1982; Al-Ansary et al., 2012).

Quartz is the primary mineral component of aeolian sands, with lesser amounts of other minerals such as feldspars and calcite reported in their composition (Abu Seif, 2013; Abu Zeid et al., 2001). The range of dry density and optimum moisture content for aeolian sands has been reported to be between 1.642 and 1.765 g/cm<sup>3</sup> and 11% to 14.5%, respectively (Al-Sanad et al.,

---

\* Corresponding author e-mail: a.cheshomi@ut.ac.ir

1993; Al-Ansary et al., 2012; Abu Zeid et al., 2001; Elipe & Lopez, 2014). Aeolian sands generally have zero cohesion and an internal friction angle between  $39^\circ$  and  $42^\circ$  (Al-Sanad et al., 1993; Al-Taie et al., 2013; Padmakumar et al., 2012). This type of soil exhibits poor geotechnical performance, particularly when not confined (Arias-Trujillo et al., 2020). The undesirable properties of aeolian sands pose significant challenges in construction. Soil improvement or stabilization has played a crucial role in civil engineering in recent years, and with the increasing demand for land reclamation and the use of lands with soft and unstable soils, its application is on the rise (Hausmann, 1990). Various methods have been proposed to enhance the engineering properties of aeolian sands. Prior to the 1990s, most laboratory studies focused on the addition of bitumen (Elipe & López, 2014). In subsequent decades, research expanded to explore different additives such as cement, cement kiln dust (CKD), bentonite, lime, bitumen emulsion, polymer emulsion, polypropylene fiber, and solid waste for improving the engineering characteristics of aeolian sands (Elipe & López, 2014).

The use of lime mortar in Asia, particularly in Iran, has a long history. Research indicates that as early as 1200 BC, Sarooj (a lime mortar composed of clay, lime, and water) was used to improve the mechanical properties of soils (Shiva Kumar & Selvaraj, 2023). For soil stabilization with lime, techniques such as adding lime powder to the soil and water, spraying a thick lime slurry onto the soil, injecting a thick lime slurry into fracture and crack systems of the mass, high-pressure lime slurry injection (Jet Grouting), and forming lime columns are employed (Das, 2016).

Similar to quicklime (pure lime, quicklime, or fired lime), calcium oxide is highly unstable and reactive, and when it absorbs water, it hydrates (Slakes). Hydrated lime ( $\text{Ca}(\text{OH})_2$ ) has much lower reactivity and is almost insoluble in water. Over time, with the absorption of carbon dioxide from the air, hydrated lime carbonates and becomes more resistant, returning to its original form (calcium carbonate) (Schotsmans et al., 2012).

For soil stabilization, lime is generally used in the form of pure calcitic lime ( $\text{CaO}$ ), pure dolomitic lime ( $\text{MgO}\cdot\text{CaO}$ ), hydrated calcitic lime ( $\text{Ca}(\text{OH})_2$ ), or hydrated dolomitic lime ( $\text{Ca}(\text{OH})_2\cdot\text{MgO}$ ) at a rate of 5 to 10 percent (Das, 2016). The addition of lime to soil has been reported to increase hardness, shear strength, unconfined compressive strength (UCS), compaction, shear resistance, California bearing ratio (CBR), tensile and flexural strength, fatigue, Poisson's ratio ( $\nu$ ), durability against freeze-thaw cycles, reduce permeability, and erosion rates of coarse-grained soils. Additionally, the impact of lime content and curing time as two significant factors in soil stabilization with lime has been investigated.

Osinubi (1998) conducted studies on the impact of increased lime on the UCS and permeability of a mixture of clay and lime, it was concluded that UCS has a direct relationship with curing time. Kazemi and Davoodi (2012) and Khalifa et al. (2010), in their studies of clay soils modified with lime, observed significant improvements in compaction, volume change, shear strength, UCS, CBR, tensile and flexural strength, fatigue,  $\nu$ , durability against freeze-thaw cycles, and permeability. Khalifa et al. (2010) also examined the effect of adding lime and other additives to cohesive clays (CH, CL) and showed that lime modification resulted in significant improvements in compaction and shear strength. Yusof et al. (2023) investigated the effect of a combination of additives (date palm fibers and hydrated lime) on the permeability of stabilized coarse-grained soils and concluded that increasing the curing time, as well as the simultaneous use of hydrated lime and date palm fibers, resulted in reduced soil permeability. A sample with 6% lime and 1.5% date palm fibers showed approximately 95% lower permeability compared to a sand sample without additives. Espitia Morales and Torres Castellanos (2022) evaluated the UCS of lime mortars (hydrated lime and sand) and demonstrated that with increased curing time, the UCS of the samples increased. Specifically, the strength of the sample after 60 days of curing was approximately twice that of the sample cured for 7 days. Banu and Attom (2023) studied the effect of lime on stabilizing coarse-grained

soils against internal erosion. The results showed that lime (CaO) is an effective agent for stabilizing sandy soils against internal erosion, and its addition significantly reduced the erosion rate, improved the Erosion Rate Index (ERI), and increased the Critical Erosion Stress (CES). Additionally, the increase in curing time of lime-stabilized soils showed a direct relationship with the ERI and CES, while it exhibited an inverse relationship with the erosion rate. Previous studies have shown that in addition to the soil-to-lime ratio, curing time, moisture content, the chemical composition of the surrounding air, and curing temperature all affect the engineering properties of lime-stabilized soil (Yusof et al., 2023; Banu & Attom, 2023; Zhang et al., 2020; Fiskvik Bache et al., 2022; Espitia Morales & Torres Castellanos, 2022). Kazemi and Davoodi (2012), who stabilized clay samples using a Saturated Lime Solution (SLS) with curing times of 3, 7, 28, and 60 days, showed that an increase in curing time resulted in an increase in the UCS of the samples. Some researchers have examined the effect of curing time and conditions on the engineering properties of lime-stabilized samples. One of the variables studied by researchers during curing is the impact of temperature. Zhang et al. (2020) investigated the effect of temperature during curing on the UCS of fine-grained soils (MH, CL, ML) stabilized with lime. Their findings showed that by increasing curing time or the amount of lime, lime stabilization could also be performed at low temperatures (below 4°C). Fiskvik Bache et al. (2022) examined the effect of temperature during curing on the strength of clay soils stabilized with lime-cement columns. The results showed that with an increase in temperature during curing, the rate of strength development significantly increased, resulting in higher strength. Salih and Abdalla (2023) studied the UCS of fine-grained soils (CL) stabilized with hydrated lime and cured at different temperatures (10 or 50°C). Their research indicated that the strength of the samples increased with higher curing chamber temperatures. Humidity and the chemical composition of the curing environment are other variables that were examined by Espitia Morales and Torres Castellanos (2022) to evaluate the UCS of lime mortars (sand and hydrated lime). They compared the UCS of samples cured in a carbonation chamber (with fixed percentages of carbon dioxide gas, humidity, and temperature at 5%, 65%, and 23°C, respectively) with samples cured in a chamber with controlled temperature and humidity (25±5°C and 55±5% humidity, respectively). Their results showed that the first set of samples had higher UCS than the second set, due to the conversion of calcium hydroxide to calcium carbonate using the carbon dioxide in the environment. Sherwood (1993) considers environmental factors such as temperature and pH to be important in the chemical interactions between lime and soil particles, which in turn affect the properties of stabilized soil. Heat, whether transient or under stable conditions, causes changes in the physical, mechanical, and microstructural characteristics of soils (Wang et al., 1990; Jefferson, 1994).

In some engineering projects, soil materials may be affected by different temperature conditions. According to previous research, soils undergo significant physical and mechanical changes under varying temperature conditions (Salih & Abdalla, 2023), making it crucial to understand the impact of temperature on soil parameters, including UCS. For example, for the safe design of oil and gas pipelines, underground high-voltage electrical cables, geothermal energy reservoirs, and nuclear waste storage tanks, it is essential to study the effect of temperature on the engineering properties of soil. Some previous studies have examined the effect of temperature on the properties of clay soils. For example, Cheshomi et al. (2020) conducted experiments to investigate the effect of temperature on the undrained shear strength ( $q_u$ ) of clay soils (Kaolinite) at temperatures ranging from 10°C to 70°C. They found that the  $q_u$  of the soil decreased with an increase in temperature. Additionally, with higher temperatures, the elastic deformation range of the samples decreased, while their plastic deformation range increased. Mohammadi et al. (2022) conducted experiments to investigate the effect of temperature on the  $q_u$  of kaolinite, illite, and montmorillonite. They demonstrated that pore water pressure is temperature-dependent and has a direct relationship with it. Additionally, the

$q_u$  and the elastic modulus (E) of the soil decreased with increasing temperature, in a linear and nonlinear manner, respectively.

Other researchers have examined the effect of temperature on the properties of granular materials. For example, Wang and Huang (2022) studied the changes in shear parameters (shear behavior, shear strength, residual shear stress) of quartz sand at high temperatures (200, 400, 600, and 800°C). Based on their results, they stated that quartz sand exposed to high temperatures tends to break more easily. Additionally, particle size significantly affects the residual shear stress and the range of changes in shear stress. Graham et al. (2004) conducted drained triaxial tests on sand within a temperature range of 27°C to 100°C and reported negligible changes in the internal friction angle ( $\phi$ ) and a 10% reduction in the shear modulus (G). Karner et al. (2005) conducted drained triaxial tests on water-saturated quartz sand at temperatures of 24°C, 150°C, and 225°C under constant average effective stress conditions. They found that the maximum deviatoric stress decreased with an increase in temperature. Yavari et al. (2016) investigated the behavior of soil and the soil-concrete interaction at different temperatures using direct shear tests. They found that the behavior of sand and clay becomes more rigid with an increase in temperature. Liu et al. (2018) studied the shear strength of sandy soil in the temperature range of 25°C to 55°C by conducting triaxial tests. They heated the samples under drained conditions and tested them under undrained conditions. The results showed that the undrained shear strength increased with the increase in average initial effective stress. However, with the rise in temperature, the shear strength decreased linearly. Punya-in and Kongkitkul (2023) conducted triaxial tests (with controlled surrounding temperature) on sand in the temperature range of 30°C to 60°C. They found that both the maximum and residual shear strength decreased with an increase in temperature. Additionally, axial strain increased with higher stress levels and temperature, while the E increased with stress but decreased with temperature. Tai et al. (2024) conducted triaxial tests under controlled temperature (ranging from 0°C to 60°C) and pressure conditions. They found that shear strength significantly increased at low confining pressure with rising temperature, while at high confining pressure, shear strength decreased.

Aeolian sand has a high relative abundance in the Khuzestan plain (Iran), making it a common source for borrow material. Research has been conducted to investigate the effect of various additives on the engineering properties of these sands. Cheshomi and Sahragard (2023) studied the aeolian sands of the Khuzestan plain, classifying them as SP and showed that adding fine-grained clay materials (CL) reduced the  $\omega_{opt}$  and increased the  $\rho_{dmax}$ . The increase in the percentage of fine particles led to an improvement in the CBR for samples prepared with natural moisture. Heravi and Cheshomi (2023, 2024) investigated the effect of polymer emulsion (Vinyl Acrylic Polymer, VAP) on the  $\rho_{dmax}$ ,  $\omega_{opt}$ , UCS, E, and shear strength parameters (C and  $\phi$ ) of aeolian sand from the Khuzestan plain. They found that adding the VAP caused little change in the  $\rho_{dmax}$ , but reduced the  $\omega_{opt}$  by 11%. The VAP with a 30% concentration and a curing time of 28 days was able to increase the UCS and E of the sample by up to two times compared to the VAP with a 10% concentration and a curing time of 7 days. Additionally, the VAP increased the shear strength of the aeolian sand by enhancing its cohesion (C).

While previous studies have explored the effects of additives and curing conditions on soil stabilization, the influence of environmental factors such as temperature has received limited attention, especially in the context of lime-stabilized sands. This study focuses on aeolian sands collected from the Khuzestan Plain an arid region characterized by high ambient temperatures and unique soil textures. The novelty of this research lies not only in the regional relevance of the studied material but also in the experimental design, which simulates field-representative temperature conditions to evaluate their impact on unconfined compressive strength (UCS). By integrating localized soil characteristics with controlled thermal curing scenarios, this work provides a deeper understanding of how temperature variations affect the performance of lime-

treated aeolian sands an area with scarce prior investigation. To achieve this, a uniaxial testing apparatus that was developed by Mohammadi et al. (2022) was utilized, and aeolian sand samples from the Khuzestan plain were stabilized with varying lime percentages. These samples were cured at a constant laboratory temperature (20°C) for different durations and subsequently tested under controlled temperature conditions to evaluate strength variations.

## Materials and Methods

### Materials

The materials used in this study include two main groups: sand (aeolian sand from the Khuzestan plain) and lime (calcium oxide powder passing through a 200-mesh sieve). The geographical location of the sample collection site is shown in Fig. 1. The chemical properties of the lime used in the study are presented in Table 1. According to the defined objectives of the research, 5%, 7%, and 9% by dry weight of lime were added to the aeolian sand. The four main soil groups used in this study are: Sand (S), sand with 5% by weight lime (S-5), sand with 7% by weight lime (S-7), and sand with 9% by weight lime (S-9).

### Methods

The methods used in the present study include grain size analysis, hydrometer test, Atterberg limits, compaction, specific gravity of solid particles ( $G_s$ ), and UCS tests. The aforementioned tests were conducted in accordance with ASTM standards.

**Table 1.** Characteristics of lime added to aeolian sand

Parameter	Value
Chemical Formula	CaO
Density (g/cm <sup>3</sup> )	3.34
Melting Point (°C)	2613
Acidity	12.8
Physical State	Solid (White Powder), Odorless
Solubility in Water	Reacts and converts to calcium hydroxide (Hydrated Lime)
Other Names	Lime, Quick Lime, Unslaked Lime, Burnt Lime, Calcium Oxide

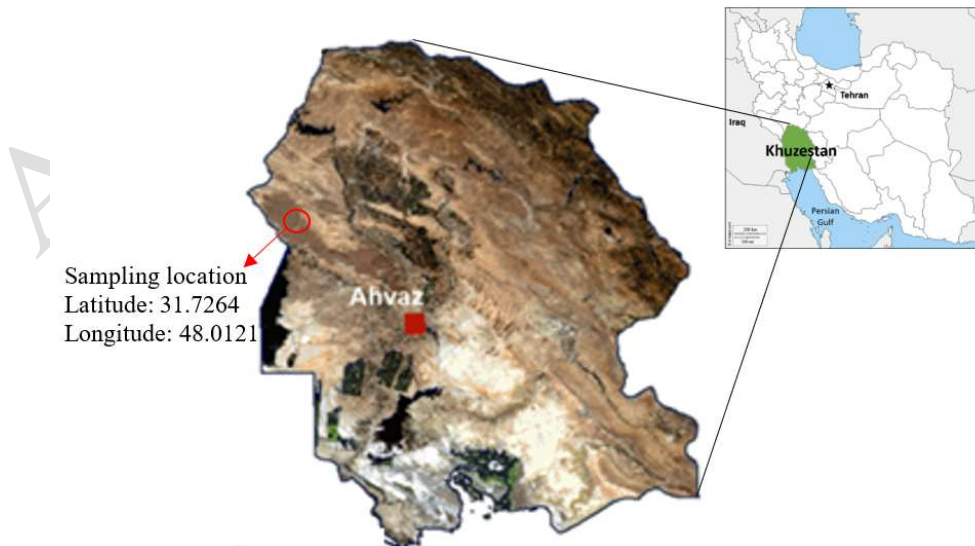


**Figure 1.** Khuzestan province map and the location of the sampling

Table 2 provides the standard test numbers along with the purpose of each test. Given that the main objective of the present study is to investigate the effect of temperature on the UCS of lime-stabilized samples, UCS tests were performed at various temperature ranges. For this purpose, a developed uniaxial testing apparatus with the capability of temperature control during the test was used, following the methodology proposed by Mohammadi et al. (2022).

The samples were prepared by mixing lime and soil (in dry form). The amount of lime added to the samples was 5%, 7%, and 9% of the total dry weight. The selection of lime contents (5%, 7%, and 9%) and the method of mixing lime with aeolian sand were based on the approach proposed by Banu and Attom (2023) and Asgari et al. (2015). Experimental results in this study showed that lime percentages below 5% had minimal impact on strength improvement, while percentages above 9% did not result in significant additional benefits. Therefore, this range was chosen to ensure an effective balance between strength enhancement and material efficiency. Following lime addition, water was introduced to the soil-lime mixture to initiate the stabilization process. The amount of water added to the mixture was selected based on the  $\omega_{opt}$  of the aeolian sand, which was obtained from the compaction test. The prepared soil was then placed inside cylindrical molds with a diameter of 3.5 cm and a length of 7 cm, where it was compacted to achieve a density equivalent to the  $\rho_{dmax}$  obtained from the compaction test. The prepared samples were cured at room temperature (20°C) for 7, 14, and 21 days. For experiments at different temperatures, a membrane was installed on the samples, and they were placed in a cell similar to the triaxial device cell (with the ability to heat the water surrounding the sample inside the cell). The stages of preparation and placement of the sample inside the cell for heating are shown in Fig. 2. Therefore, the samples were dry when they were placed inside the cell for heating.

According to the method proposed by Mohammadi et al. (2022), after placing the sample inside the cell for heating, the temperature was increased in 5°C steps. At each step, the temperature was kept constant for 10 minutes to ensure thermal equilibrium between the sample and the surrounding water. Then, the next temperature step was applied, increasing the temperature by 5°C compared to the previous step. At the final temperature step, the temperature was maintained for 30 minutes to ensure thermal equilibrium between the sample and the surrounding water.

**Table 2.** Number and type of tests conducted in the present study along with their corresponding standard numbers.

Row	Laboratory Tests	Purpose of Test	Standard Test Number	Number of Tests
1	Grain size analysis	Soil classification based on particle size and plasticity behavior	ASTM D 422-63(2017)	1
2	Hydrometer test	Soil classification	ASTM D7928-21e1(2021)	1
3	Atterberg limits	Soil classification	ASTM D4318-17e1(2018)	1
4	Specific gravity of solid particles ( $G_s$ )	Converting soil volume to weight	ASTM D 854-87 (2014)	1
5	Standard proctor compaction	Determining the maximum dry density ( $\gamma_{dmax}$ ) and optimum moisture content ( $\omega_{opt}$ ) of aeolian sand	ASTM D698-12(2021)	1
6	Unconfined compressive strength (UCS) under various temperature conditions	Investigating the effect of temperature on the $q_u$ of samples	ASTM D2166/D2166M-16, Method proposed by Mohammadi et al. (2022)	192
7	SEM Imaging	Investigating the internal structure of the samples and the interaction between components (sand and lime)	-	16

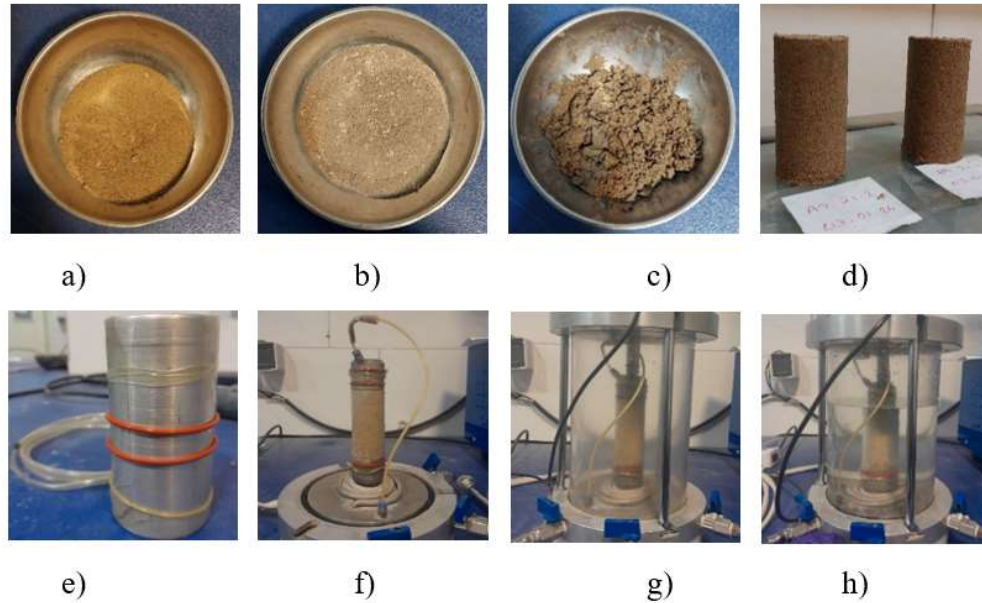


**Figure 2.** Stages of sample preparation: a) Base soil (aeolian sand from the Khuzestan plain), b) Mixing the base soil with lime in a dry form, c) Adding water and homogenizing the mixture, d) Cylindrical samples made for unconfined compressive strength testing, e) The membrane along with the sample, f) Sample with membrane, g) Sample placed inside the cell for heating, h) Adding water around the sample to transfer heat during the test

As stated in the materials section, the materials used in this study include aeolian sand and three other groups produced by mixing aeolian sand with varying percentages of lime. To identify the samples, since the samples in this study are aeolian sand, the letter "S" was used. The first number after the letter represents the dry weight percentage of lime added to the aeolian sand, and the second number indicates the curing time. The third number represents the temperature at which the sample was tested. For example, the sample marked as S-5-7(20) is a sample that contains 5% lime, has a curing time of 7 days, and was tested at a temperature of 20°C.

### The results and their analysis

The particle size distribution curve of the base soil used in the present study is shown in Fig. 3a. Based on this curve, the aeolian sand used is classified as SP (poorly graded sand) according to the USCS. The compaction curve of the aeolian sand is shown in Fig. 3b. Based on this curve, the  $\rho_{dmax}$  of the sample is 1.688 g/cm<sup>3</sup>, and its  $\omega_{opt}$  is 13.18%.

Unconfined compressive strength tests were conducted to determine the maximum unconfined compressive strength ( $q_u$ ) on the samples used in the present study. The base soil is aeolian sand without any additives. Due to the absence of fine particles, this soil is non-cohesive, and it is not possible to form cylindrical samples for determining the  $q_u$ . Fig. 4 shows stress-strain curves obtained from UCS test on aeolian sand samples S-9-21, S-7-21 and S-5-21 at different temperatures. The stress-strain diagrams for the other samples presented in Table 3 were also plotted.

The stress-strain curves show similar behavior for the samples stabilized with different lime percentages at various temperatures. The behavior of all the samples is brittle, in that after reaching the maximum point, they rapidly lose their strength, and no residual strength is observed in the samples. As the temperature increases from 20°C to 70°C, it is observed that the samples reach their maximum stress at lower strains. This indicates that with higher

temperatures, the sample becomes more brittle, and its strength decreases. Slight variations in the slope of the curves are observed however, with increasing temperature, the samples reach the failure point at lower strains indicating a decrease in strength and an increase in brittleness with higher temperatures. The maximum point on these curves is defined as the  $q_u$ , and the corresponding values for the samples used in the present study are presented in Table 3.

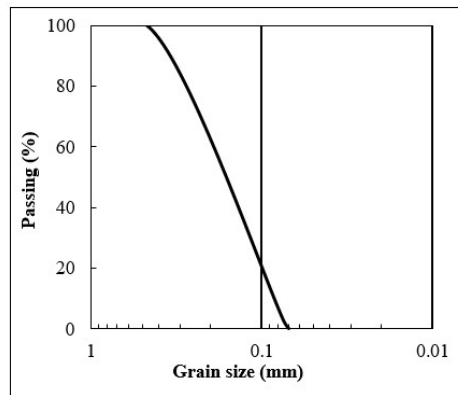
In Fig. 5 (a, b, c, and d), the  $q_u$  of aeolian sand samples stabilized with 5%, 7%, and 9% lime and cured for 7, 14, and 21 days is presented for temperatures of 20, 30, 50, and 70°C, based on the results provided in Table 3.

Fig. 5a shows the results for samples tested at 20°C. In these samples, for a given lime percentage,  $q_u$  decreases with decreasing curing time. On the other hand, for a given curing time,  $q_u$  increases with the increase in lime percentage. Therefore, it can be concluded that when the tests are conducted at laboratory temperature (20°C), there is a direct relationship between  $q_u$  of the samples, the additive percentage, and the curing time.

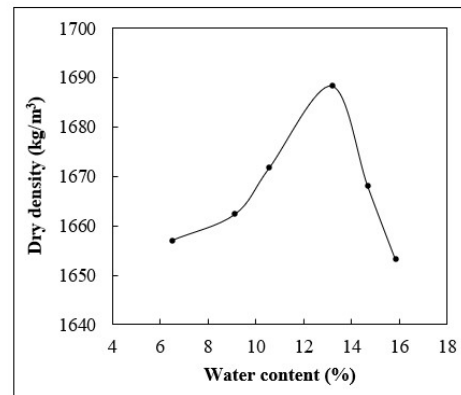
Fig. 5b shows the results for samples tested at 30°C. For a given lime percentage,  $q_u$  decreases with decreasing curing time. However, the rate of decrease is less compared to the samples tested at laboratory temperature. The reduction in strength with decreasing curing time is minimal for the samples stabilized with 5% lime and tested at 30°C. Therefore, curing time had no significant effect on the  $q_u$  of the samples stabilized with 5% lime and tested at 30°C.

**Table 3.** Maximum  $q_u$  for the samples

Sample ID.	$q_u$ (kN/m <sup>2</sup> )	Sample ID.	$q_u$ (kN/m <sup>2</sup> )	Sample ID.	$q_u$ (kN/m <sup>2</sup> )
1 S-5-7(20)	442.31	13 S-7-7(20)	531.63	25 S-9-7(20)	564.00
2 S-5-7(30)	354.19	14 S-7-7(30)	357.42	26 S-9-7(30)	391.96
3 S-5-7(50)	285.59	15 S-7-7(50)	340.00	27 S-9-7(50)	370.92
4 S-5-7(70)	221.34	16 S-7-7(70)	332.39	28 S-9-7(70)	321.72
5 S-5-14(20)	496.08	17 S-7-14(20)	645.79	29 S-9-14(20)	688.87
6 S-5-14(30)	360.45	18 S-7-14(30)	402.74	30 S-9-14(30)	455.29
7 S-5-14(50)	315.24	19 S-7-14(50)	382.76	31 S-9-14(50)	390.51
8 S-5-14(70)	236.00	20 S-7-14(70)	350.76	32 S-9-14(70)	337.68
9 S-5-21(20)	570.03	21 S-7-21(20)	684.14	33 S-9-21(20)	737.00
10 S-5-21(30)	362.71	22 S-7-21(30)	431.38	34 S-9-21(30)	490.68
11 S-5-21(50)	327.15	23 S-7-21(50)	417.82	35 S-9-21(50)	410.76
12 S-5-21(70)	250.86	24 S-7-21(70)	358.51	36 S-9-21(70)	350.76



a)



b)

**Figure 3.** a) Particle size distribution curve and (b) variation in dry density with respect to moisture content for the aeolian sand

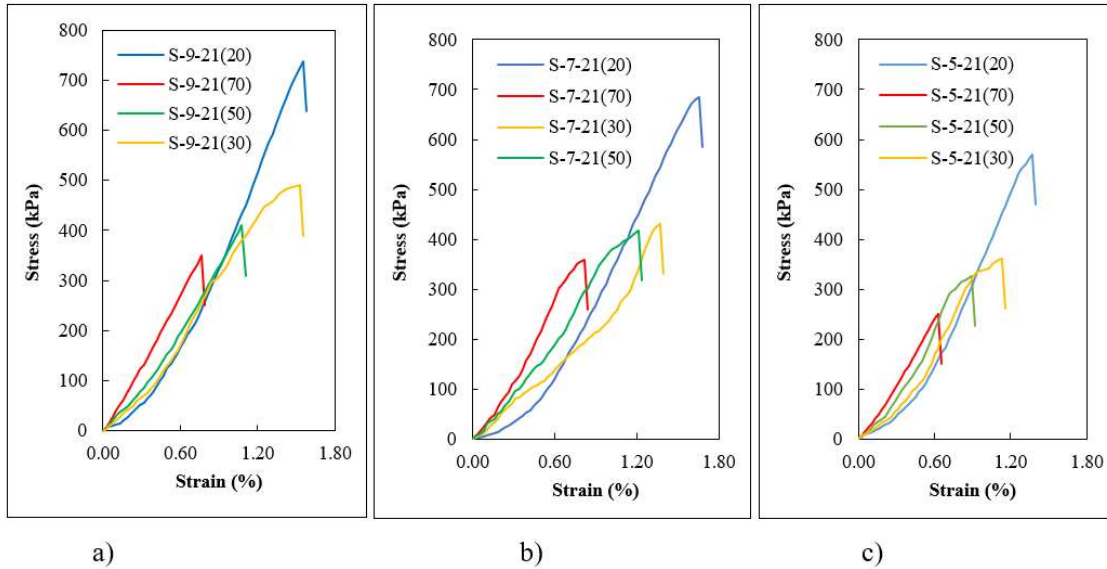


**Figure 4.** Stress-strain curves at different temperatures for samples a) S-9-21, b) S-7-21, c) S-5-21

Fig. 5c and 5d show the trend of decreasing  $q_u$  with decreasing curing time for samples tested at 50°C and 70°C. A similar decreasing trend in strength with decreasing curing time and increasing lime percentage is also observed for these two temperatures. However, the rate of decrease is less pronounced compared to the samples tested at 20°C and 30°C.

In all samples, a reduction in  $q_u$  is observed with a decrease in lime percentage. Therefore, it can be concluded that a nearly similar trend between the changes in lime percentage and curing time is observed for samples tested at different temperatures, but the measured  $q_u$  values differ across the various temperatures.

Since the main objective of the present study is to examine the effect of temperature on the  $q_u$  of lime-stabilized aeolian sand, Fig. 6 shows the variations in  $q_u$  of the samples with temperature. Fig. 6 (a, b and c) represent the samples stabilized with 9%, 7%, and 5% lime, respectively, with curing times of 7, 14, and 21 days. In all three graphs,  $q_u$  decreases with increasing temperature. The rate of decrease in  $q_u$  with rising temperature varies for the samples stabilized with different lime percentages, such that for samples with higher lime percentages, the decrease in  $q_u$  with increasing temperature is more pronounced.

To investigate the possibility of a logical relationship between temperature changes and the  $q_u$  of various samples, Fig. 7 (a, b, and c) show the curves of  $q_u$  variations with temperature for samples stabilized with 9%, 7%, and 5% lime at different curing times under various temperature conditions. These graphs suggest that it is possible to propose an empirical relationship between  $q_u$  and temperature for each group of samples, as outlined in Table 4. The coefficient of correlation ( $R$ ) of the empirical relationships presented in Table 3 ranges from 0.85 to 0.99, indicating a good correlation between the  $q_u$  of the lime-stabilized samples with different lime percentages and temperature. Each relationship is provided for a specific lime percentage and curing time. Clearly, the relationships are valid within the temperature and additive percentage ranges of the present study.

By combining Fig. 7 (a, b, and c), Fig.8 can be derived. In this figure, a range can be defined based on the results obtained in the present study. The upper limit of the range corresponds to the sample stabilized with 9% lime and cured for 21 days (S-9-21), which shows the highest  $q_u$  at various temperatures. At 20°C, the  $q_u$  of this sample is 737 kPa. As the temperature increases, the strength of this sample decreases, reaching 370 kPa at 70°C. A 50% decrease in  $q_u$  is observed with a 50°C increase in temperature. The lower limit of the range corresponds to the sample stabilized with 5% lime and cured for 7 days (S-5-7), which shows the lowest  $q_u$  at

various temperatures. The  $q_u$  of this sample at 70°C is measured as 221 kPa. When tested at 20°C, the  $q_u$  of this sample is 442 kPa, and a 50% decrease in strength is also observed due to the 50°C increase in temperature.

**Table 4.** Proposed empirical relationships between  $q_u$  and temperature for samples stabilized with different lime percentages

Eq. No.	Sample ID.	Lime content (%)	Curing time (days)	Equation	R
1	S-9-7	9	7	$q_u = 3162.4T^{-0.535}$	0.96
2	S-9-14		14	$q_u = 1748.7T^{-0.403}$	0.93
3	S-9-21		21	$q_u = 3690.7T^{-0.562}$	0.97
4	S-7-7	7	7	$q_u = 1329T^{-0.342}$	0.85
5	S-7-14		14	$q_u = 2133.4T^{-0.439}$	0.88
6	S-7-21		21	$q_u = 2414.1T^{-0.456}$	0.91
7	S-5-7	5	7	$q_u = 2191.6T^{-0.533}$	0.99
8	S-5-14		14	$q_u = 2474.8T^{-0.546}$	0.98
9	S-5-21		21	$q_u = 3127.4T^{-0.593}$	0.96

$q_u$ : kPa and T is temperature (°C)

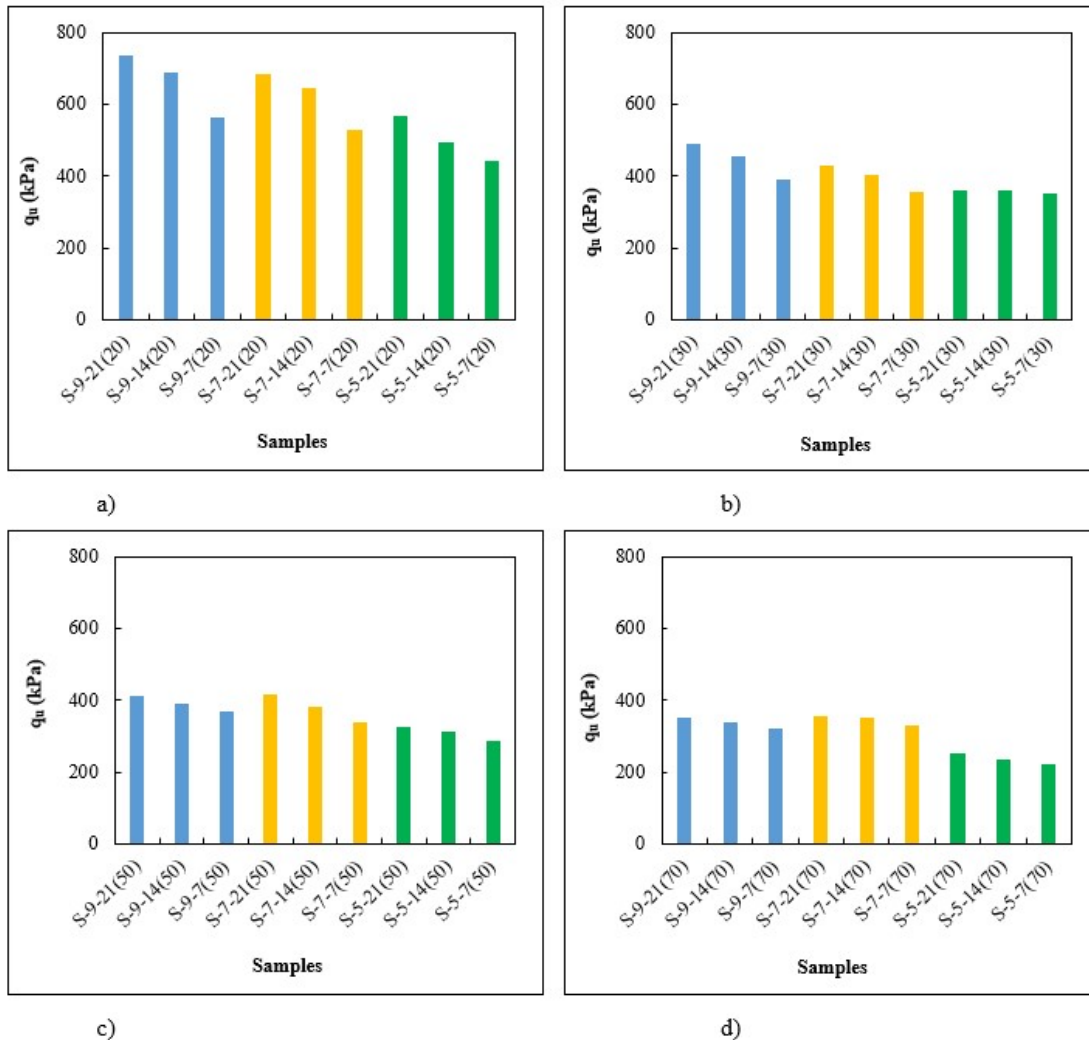


**Figure 5.** Comparison of  $q_u$  of samples with different lime percentages and curing times at the following temperatures: a) 20°C, b) 30°C, c) 50°C, and d) 70°C

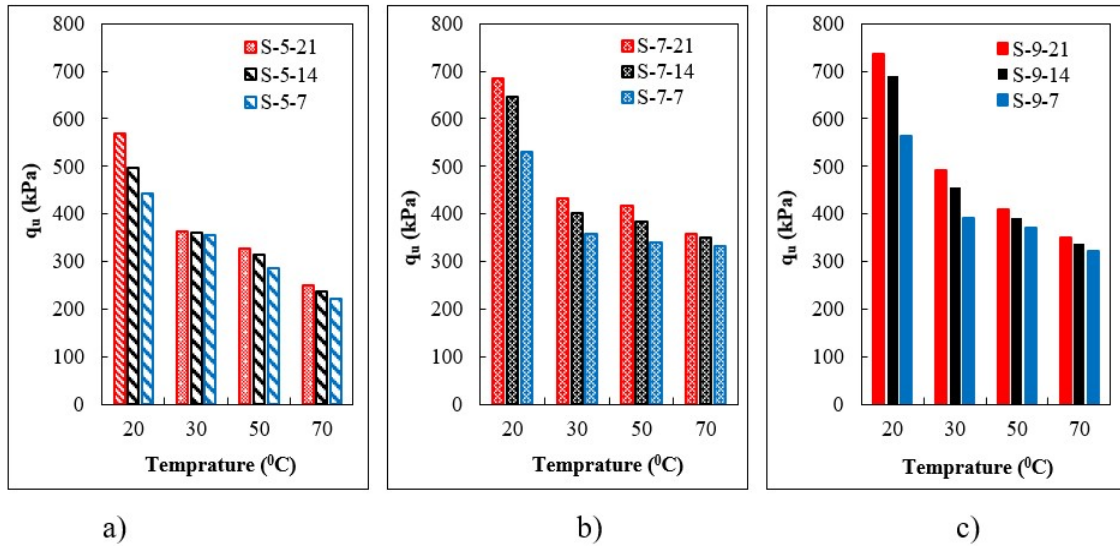


**Figure 6.** Comparison of  $q_u$  of samples at different temperatures for samples stabilized with (a) 5%, (b) 7%, and (c) 9% lime at different curing times

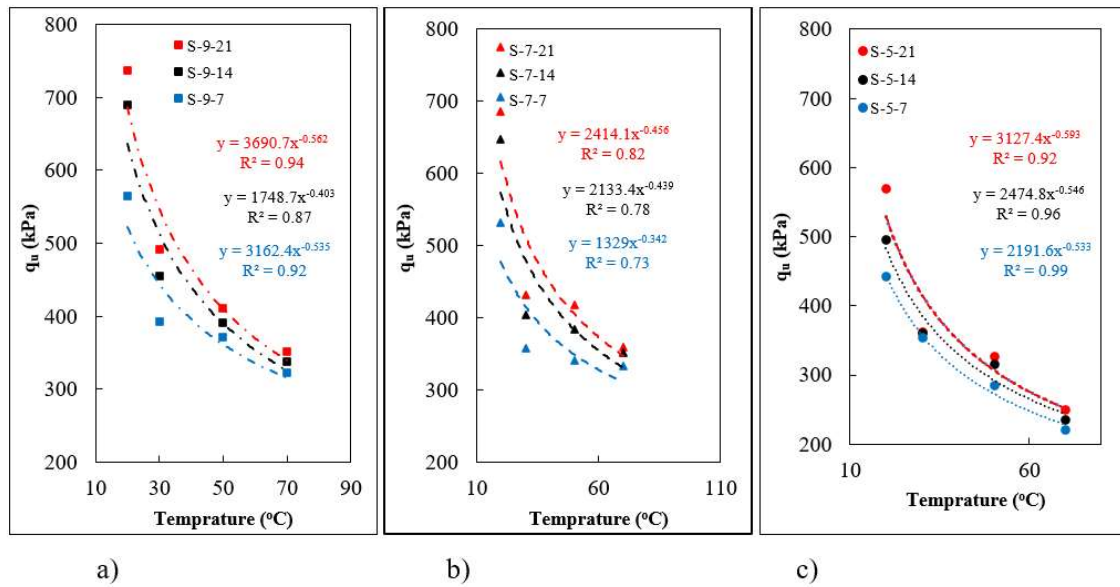


**Figure 7.** Curves of  $q_u$  versus temperature with different curing times, for a) 9%, b) 7%, and c) 5% lime

In order to assess the possibility of establishing an empirical relationship between the various variables investigated in the present study, multiple linear regression analysis was performed using SPSS software. Based on this, it is possible to propose the empirical relationship (Eq. 10) between the  $q_u$ , the sample temperature at the time of testing, curing time, and lime additive percentage within the range of experiments conducted in the present study.

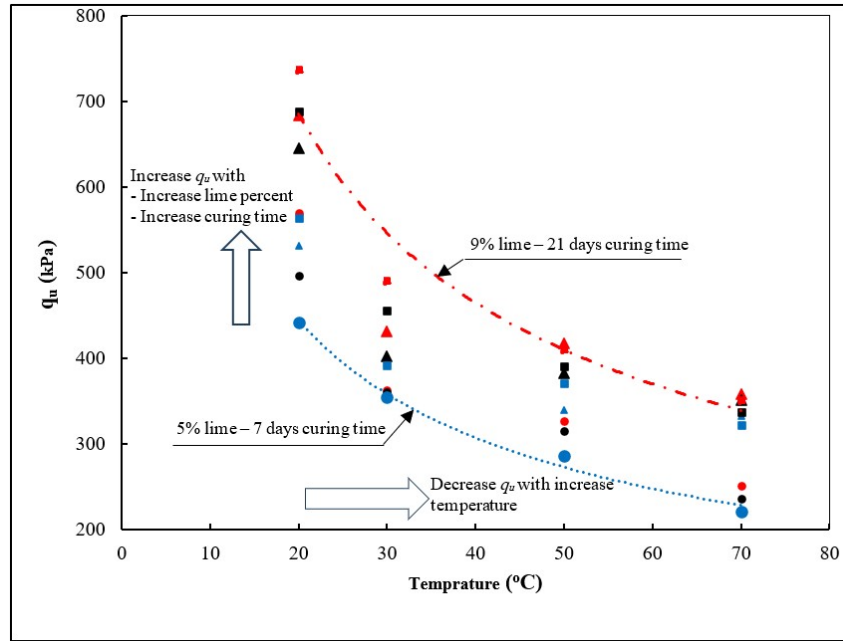
$$q_u = 364.32 - 4.93 T + 5.23 C + 26.84 L \quad (10)$$

In Eq. 10,  $q_u$  is in kPa,  $T$  is the temperature in °C,  $C$  is the curing time in days, and  $L$  is the weight percentage of lime added to the aeolian sand.

The statistical parameters related to Eq. 10 are provided in Table 5. Based on the data in Table 5, the coefficient of correlation ( $R$ ) for the equation is 0.87.

**Table 5.** Statistical parameters of the proposed model for equation 10

R	R <sup>2</sup>	Adjuster R <sup>2</sup>	Standard error the estimate	F change	df1	df2	Sig. F change
0.866	0.750	0.727	66.47	32	3	32	<0.001

**Figure 8.** Range of variations in  $q_u$  for samples stabilized with 5%, 7%, and 9% lime at curing times of 7, 14, and 21 days under different temperatures

In Fig. 9 the measured  $q_u$  from the uniaxial test are compared with estimated  $q_u$  from Eq. 10. As expected, the data points closely align with the one-to-one line, confirming a good fit between the measured and estimated  $q_u$ . The upper and lower bounds of the data points are also shown in this figure, highlighting the range of variability around the one-to-one line. The closeness of the values to the one-to-one line indicates that the Eq. 10 is capable of estimating the  $q_u$  of aeolian sand stabilized with different lime percentages and curing times under various temperatures within the range of experiments conducted in the present study. Furthermore, based on the statistical parameters provided in Table 4, the estimation error of the relationship is determined to be 66.47 MPa, which is indicated by the ranges shown above and below the one-to-one line in Fig. 9.

## Discussion

Previous studies conducted in various regions worldwide have shown that aeolian sands are classified as *SP* according to the USCS (Khan, 1982; Al-Sanad et al., 1993; Abu Zeid et al., 2001; Al-Ansary et al., 2012; Elipe and Lopez, 2014; Arias Trujillo et al., 2020; Souza Júnior et al., 2020). Based on the results of the particle size distribution test, the aeolian sands of the Khuzestan plain also fall into the *SP* category. The  $\gamma_{dmax}$  and  $\omega_{opt}$  of the Khuzestan plain aeolian sand are within the range of  $\gamma_{dmax}$  and  $\omega_{opt}$  reported in previous studies (Al-Sanad et al., 1993; Al-Ansary et al., 2012; Abu Zeid et al., 2001; Elipe and Lopez, 2014).

The increase in the strength of granular materials with the addition of lime and the extension of curing time has previously been reported by Asgari et al. (2003), Moayed et al. (2012), and Yusof et al. (2023). In the present study, this finding was also concluded for samples stabilized with 5%, 7%, and 9% lime and cured for 7, 14, and 21 days.

The validation of empirical Eq. 10 was conducted by performing tests on six samples with the specifications provided in Table 6. The preparation and testing conditions for the samples in Table 6 were similar to those used for the other samples. The measured  $q_u$  values obtained from the tests and the estimated values from the Eq.10 for these samples are presented in Table 6.

The values of absolute error and relative error for each test were calculated using Eqs. 11 and 12 and are presented in Table 6. The average absolute error for the six validation tests is 29.29 kPa, and the average relative error is 7.81%. Given that the average relative error is less than 10%, it can be concluded that the proposed equation in this study can estimate the  $q_u$  of aeolian sand samples stabilized with different lime percentages and curing times at various temperatures with reasonable accuracy. It is important to note that the proposed equation is valid within the range of soil types, temperatures, lime percentages, and curing times considered in this study, and its applicability to other conditions requires further testing. In Figs. 10 and 11, the validation test results are plotted on measured  $q_u$  versus estimated  $q_u$  and  $q_u$  versus Temperature diagrams, demonstrating that the validation tests fall within the predicted ranges.

$$\text{Absolute Error} = |\text{Estimated Value} - \text{Measured Value}| \quad (11)$$

$$\text{Relative Error} = \left( \frac{\text{Absolute Error}}{\text{Estimated Value}} \right) \times 100 \quad (12)$$

**Table 6.** Sample characteristics and test results for validation

Sample	Est. UCS	Mes. UCS	Absolute Error	Relative Error
S-6-7(40)	364.77	386	21.23	5.82
S-6-21(40)	437.99	470	32.01	7.31
S-8-14(40)	455.06	421	34.06	7.48
S-6-14(60)	302.78	332	29.22	9.65
S-8-7(60)	319.85	346	26.15	8.18
S-8-21(60)	393.07	360	33.07	8.41
		Average	29.29	7.81

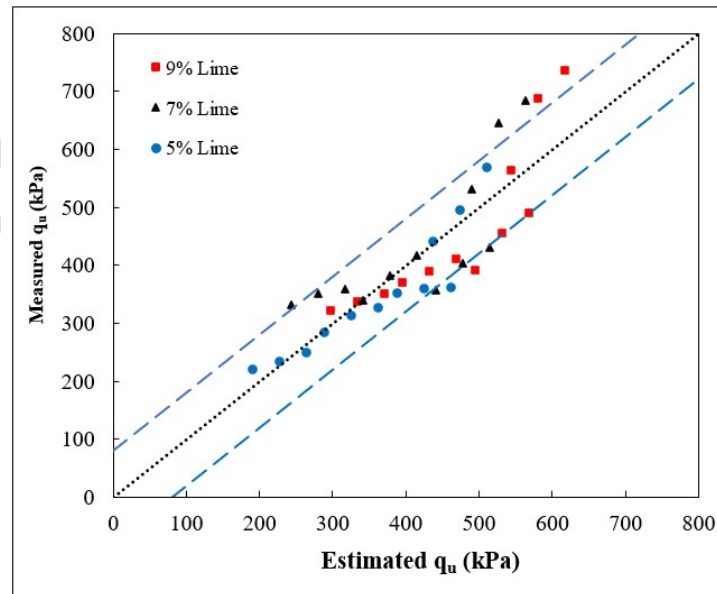


**Figure 9.** Measured and estimated  $q_u$  based on the proposed statistical model with Eq. 10

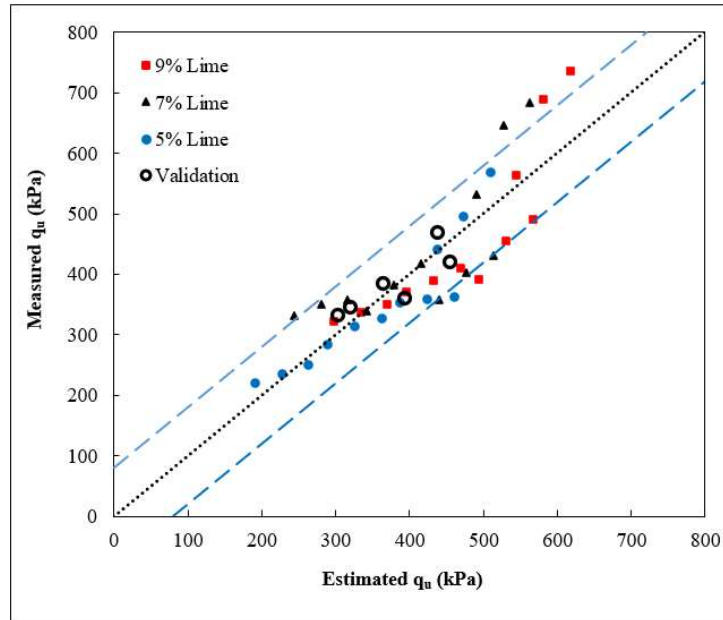


Figure 10. Position of validation samples on the estimated vs. measured  $q_u$  diagram

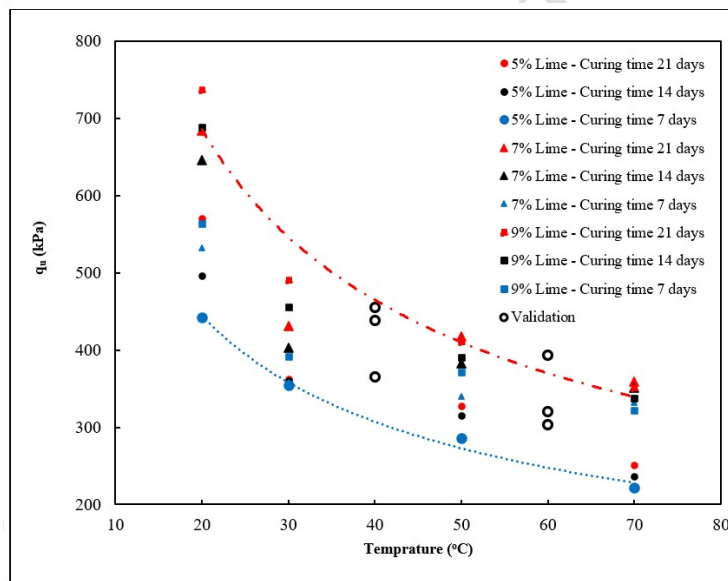


Figure 11. Position of validation samples on the  $q_u$  vs. temperature diagram

To quantify and determine the percentage variation in the  $q_u$  of the samples, the parameter  $\alpha$  is defined as per Eq. 13.

$$\alpha = \frac{q_u}{q_{u(\min)}} \times 100 \quad (13)$$

Where  $\alpha$  represents the percentage variation in unconfined compressive strength,  $q_u$  is the measured UCS for each sample as listed in Table (3), and  $q_{u(\min)}$  is the minimum measured UCS among the samples.

As previously mentioned, since it was not possible to determine the  $q_u$  of untreated aeolian sand due to the inability to prepare cylindrical specimens, the minimum measured  $q_u$  from the tests is 221.34 kPa, corresponding to sample S-5-7(70) was considered as  $q_{u(\min)}$ .

In Fig. 12, the variations in  $\alpha$  for the samples stabilized with different lime percentages and

subjected to different curing times at various temperatures are shown. For the samples stabilized with 9% lime at different curing times and temperatures (Fig.12a), the highest  $\alpha$  value is 3.32, which corresponds to the sample cured for 21 days and tested at 20°C, while the lowest  $\alpha$  value is 1.45, which corresponds to the sample cured for 7 days and tested at 70°C. For the samples stabilized with 7% lime at different curing times and temperatures (Fig. 12b), the highest  $\alpha$  value is 3.09, corresponding to the sample cured for 21 days and tested at 20°C, while the lowest  $\alpha$  value is 1.50, corresponding to the sample cured for 7 days and tested at 70°C.

For the sample stabilized with 5% lime at different curing times and temperatures (Fig. 12c), the highest  $\alpha$  value is 2.57, which corresponds to the sample cured for 21 days and tested at 20°C, while the lowest  $\alpha$  value is 1, corresponding to the sample cured for 7 days and tested at 70°C. Therefore, increasing the temperature to 70°C can reduce the  $q_u$  of the sample by up to 3.32 times.

The increase in  $q_u$  due to lime addition in aeolian sand can be attributed to the formation of interparticle bonds facilitated by lime particles. As observed in the electron microscope images (Fig. 13), lime particles are present on the surface of sand grains, filling the voids within the sample and creating cohesive links between particles. Although these bonds may initially be weak, they strengthen over time, leading to a progressive increase in strength with higher lime content. This bonding mechanism explains the observed improvement in the mechanical behavior of lime-stabilized samples.

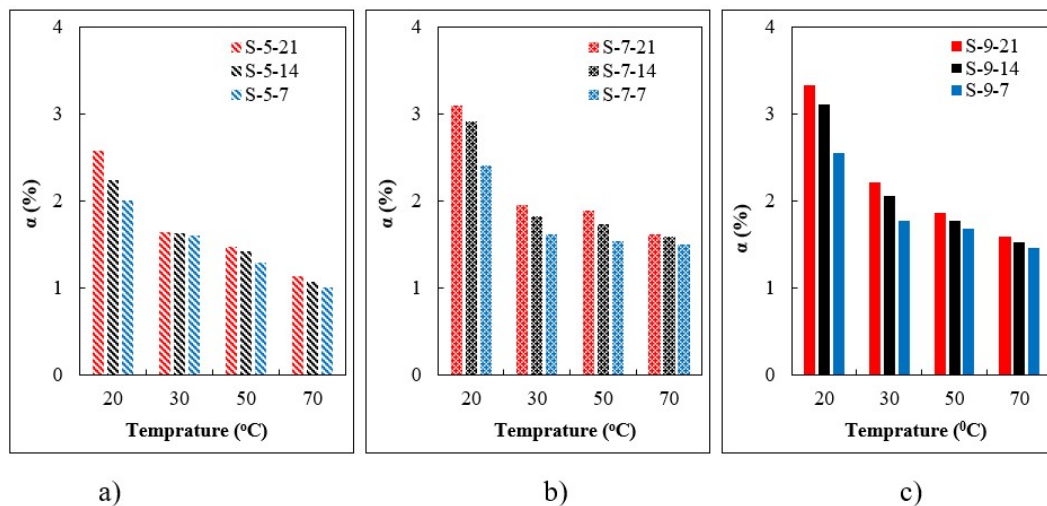


**Figure 12.** Variations of the coefficient  $\alpha$  for samples stabilized with: a) 5%, b) 7%, c) 9% lime at different curing times and temperatures.

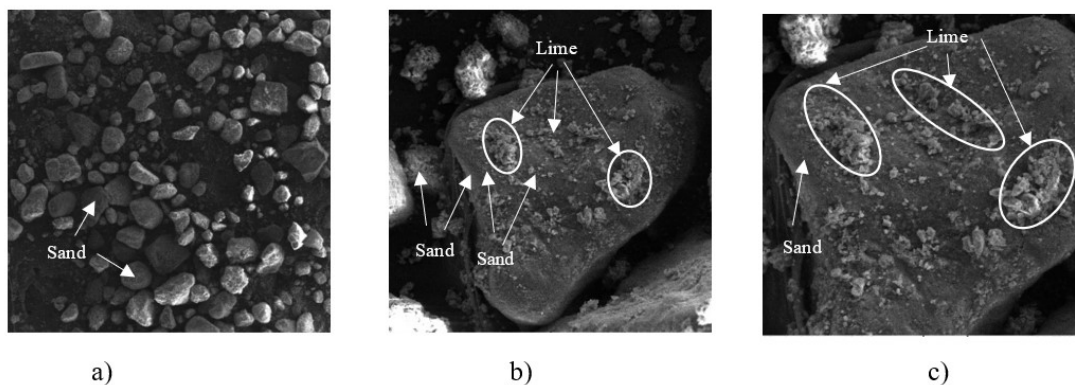


**Figure 13.** Electron microscope images of the sample stabilized with 9% lime and cured for 21 days, showing magnifications of: a) 100x, b) 1000x, c) 1500x

The type of soil, the type of test chosen to determine the strength, the saturation and moisture conditions of the sample, the drainage or undrained test conditions, and the soil composition all influence how temperature affects the sample's strength (Yavari et al., 2016). Most studies conducted on the effect of temperature on soil strength have focused on fine and coarse-grained soils, and examining the effect of temperature on the  $q_u$  of lime-stabilized aeolian sand for specific area (Khuzestan Plain) is a novel aspect of the present research. The reduction in  $q_u$  due to increasing temperature in fine-grained materials has been reported by Cheshomi et al. (2020), De Bruyn and Thimus (1996), Laloui (2001), Yu et al. (2018), and Ma et al. (2020).

Pore pressure consists of two components: pore water pressure and pore air pressure. Given that the samples were dry during testing, the voids between the particles can be considered as filled with air and a small amount of hygroscopic water. The difference in the thermal expansion coefficients of sand grains and lime particles, coupled with the increase in the kinetic energy of the air between the grains due to the rise in temperature, could be a reason for the decrease in the  $q_u$  of the samples.

Zhao et al. (2022) attribute the formation of cracks at the interface of different materials to differences in their thermal expansion coefficients. According to this, differences in the values of these coefficients in the components of soil or similar mixtures lead to heterogeneous changes in the dimensions of the components, weakening the internal structure of the mixture, and ultimately reducing its strength. The thermal expansion coefficient of sand (quartz sand) ranges from  $9.9 \times 10^{-6}$  to  $12.8 \times 10^{-6}$  per degree Celsius, while the thermal expansion coefficient of lime is  $1.4 \times 10^{-6}$  per degree Celsius (Neville, 2011). This tenfold difference (approximately  $9.5 \times 10^{-6}$  per degree Celsius on average) between the thermal expansion coefficients of these two materials causes differences in their expansion rates and, consequently, their separation, which leads to a decrease in the strength of the mixture due to increased temperature. In the case of concrete, if the difference in the thermal expansion coefficient between the aggregate and the cement paste exceeds  $5.5 \times 10^{-6}$  per degree Celsius, the durability of the concrete under freeze-thaw cycles is affected (Neville, 2011).

Haravi and Cheshomi (2023) investigated the effect of VAP on the unconfined compressive strength ( $q_u$ ) of aeolian sand from the Hoor al-Azim region at laboratory temperature. Their study found that adding 30% VAP with a curing time of 21 days increased the  $q_u$  of the sand to 808 kPa. In contrast, the present study showed that adding 9% lime with a curing time of 21 days at laboratory temperature increased the  $q_u$  of aeolian sand to 737 kPa. These results suggest that, for a given curing time, the effect of approximately 10% VAP on increasing  $q_u$  is more significant than that of lime.

## Conclusion

In this study, the effect of temperature on the unconfined compressive strength ( $q_u$ ) of lime-treated aeolian sand was investigated. For this purpose, after sampling from the aeolian sand in the Khuzestan plain and performing identification tests to determine the  $\omega_{opt}$  and  $\gamma_{dmax}$ , different percentages (5%, 7%, and 9%) of lime (calcium oxide) were added to the base soil. The samples were cured in a laboratory temperature (20 °C) for 7, 14, and 21 days. The  $q_u$  of the different samples was determined under varying temperature (20, 30, 50, and 70 °C). The findings of this research are as follows:

The stress-strain curves for different samples were similar, such that changes in the percentage of lime, curing time, and temperature did not significantly affect the overall shape of the curves. All samples exhibited brittle behavior, showing a sharp increase in strength until reaching the maximum strength, after which they did not show any residual strength.

As the temperature increases from 20°C to 70°C, the samples reach their maximum stress at lower strains. This indicates that with higher temperatures, the sample becomes more brittle,

and its strength decreases.

For all samples, an increase in the percentage of lime and curing time resulted in an increase in  $q_u$ . The trend of changes in  $q_u$  with respect to lime percentage and curing time is nearly linear.

A significant decrease in  $q_u$  of the samples was observed with increasing temperature. Specifically, an increase in temperature from 20°C to 70°C resulted in an average reduction of 50% in the strength of the samples. The curve of changes in  $q_u$  with temperature was nonlinear, and empirical relationships between  $q_u$  and temperature were proposed for samples stabilized with different percentages of lime and various curing times.

Given that the samples were dried after curing, the decrease in  $q_u$  of the samples can be attributed to the difference in the thermal expansion coefficients of lime and sand, as well as the pressure caused by the increased volume of air between the particles of the samples.

A range is defined to show the changes in the  $q_u$  of the samples tested in the present study against temperature, such that the upper limit of this range corresponds to a sample that was stabilized with 9% lime and cured for 21 days, while the lower limit corresponds to a sample that was stabilized with 5% lime and cured for 5 days.

An empirical relationship for estimating the  $q_u$  of the samples at varying temperature, curing time, and different lime additive percentages within the range of experiments conducted in the present study was proposed.

SEM images confirmed the presence of lime particles on the surfaces of the sand grains and within the voids between them. These lime particles fill the spaces between the grains, contributing to increased soil compaction and subsequently enhancing the  $q_u$  of the samples

### **Conflicts of interest**

The authors declare that there is no conflict of interest regarding the publication of this manuscript.

### **Authors' contributions**

Akbar Cheshomi: Conceptualization, Methodology, Supervision, Writing - Review & Editing, Visualization, Project administration, Funding acquisition. Farnaz Safarzadeh: Formal analysis, Data Curation, Writing - Original Draft, Investigation.

### **References**

- Abu Seif, E.S., 2013. Performance of cement mortar made with fine aggregates of dune sand, Kharga Oasis, Western Desert, Egypt: an experimental study. *Jordan Journal of Civil Engineering*, 7(3): 270-84.
- Abu-Zeid, M.M., Baghdady, A.R., El-Etr, H.A., 2001. Textural attributes, mineralogy and provenance of sand dune fields in the greater Al Ain area, United Arab Emirates. *Journal of Arid Environments*, 48(4): 475-499.
- Al-Ansary, M., Pöppelreiter, M.C., Al-Jabry, A., Iyengar, S.R., 2012. Geological and physiochemical characterisation of construction sands in Qatar. *International Journal of Sustainable Built Environment*, 1(1): 64-84.
- Al-Sanad, H.A., Ismael, N.F., Nayfeh, A.J., 1993. Geotechnical properties of dune sands in Kuwait. *Engineering Geology*, 34(1-2): 45-52.
- Al-Taie, A.J., Al-Shakarchi, Y.J., Mohammed, A.A., 2013. Investigation of geotechnical specifications of sand dune soil: a case study around Baiji in Iraq. *IJUM Engineering Journal*, 14(2).
- Arias-Trujillo, J., Matias-Sanchez, A., Cantero, B., López-Querol, S., 2020. Effect of polymer emulsion on the bearing capacity of aeolian sand under extreme confinement conditions. *Construction and Building Materials*, 236: 117473.
- ASTM D422-63, 2017. Standard test method for particle-size analysis of soils. West Conshohocken PA.

- ASTM D7928-21e1, 2021. Standard test method for particle-size distribution (gradation) of fine-grained soils using the sedimentation (hydrometer) analysis. West Conshohocken PA.
- ASTM D4318-17e1, 2018. Standard test methods for liquid limit, plastic limit, and plasticity index of soils. West Conshohocken PA.
- ASTM 854-14, 2014. Standard test methods for specific gravity of soil solids by water pycnometer. West Conshohocken PA.
- ASTM D698-12, 2021. Standard test methods for laboratory compaction characteristics of soil using standard effort (12,400 ft-lbf/ft<sup>3</sup> (600 kN-m/m<sup>3

ASTM D2166/D2166M-16, 2024. Standard test method for unconfined compressive strength of cohesive soil. West Conshohocken PA.

Asghari, E., Toll, D.G. Haeri, S.M., 2003. Triaxial behaviour of a cemented gravely sand, Tehran alluvium. *Geotechnical and Geological Engineering*, 21: 1-28.

Asgari, M.R., Baghebanzadeh Dezfali, A., Bayat, M., 2015. Experimental study on stabilization of a low plasticity clayey soil with cement/lime. *Arabian Journal of Geoscience*, 8: 1439-1452.

Banu, S.A., Attom, M.F., 2023. Effect of curing time on lime-stabilized sandy soil against internal erosion. *Geosciences*, 13: 102.

Cheshomi, A., Mohammadi, F., Rajabi, A.M., 2020. Investigation of the effect of temperature on the undrained shear strength of kaolinite. *Amirkabir Journal of Civil Engineering*, 52(8): 1971-1982.

Cheshomi, A., Sahragard, A., 2023. Use of fine-grained soil for improvement of density and bearing capacity of aeolian sand. *Geopersia*, 13(2): 261-274.

Das, Braja M., 2016. *Principle of Foundation Engineering*. 8th Edition, Cengage Learning. 896pp.

De Bruyn, D., Thymus, J.F., 1996. The influence of temperature on mechanical characteristics of Boom clay: The results of an initial laboratory programme. *Engineering Geology*, 41:117-123.

Elipe, M.G.M., L'opez-Querol, S., 2014. Aeolian sands: characterization, options of improvement and possible employment in construction - the state-of-the-art. *Construction and Building Materials*, 73(12): 728-739.

Espitia-Morales, A.F., Torres-Castellanos, N., 2022. Assessment of the compressive strength of lime mortars with admixtures subjected to two curing environments. *Ingeniería e Investigación*, 42(2): e91364. <http://doi.org/10.15446/ing.investig.91364>.

Fiskvik Bache, B.K., Wiersholm, P., Paniagua, P., Emdal, A., 2022. Effect of temperature on the strength of lime-cement stabilized Norwegian clays. *Journal of Geotechnical and Geoenvironmental Engineering*, 148(3) [https://doi.org/10.1061/\(ASCE\)GT.1943-5606.0002699](https://doi.org/10.1061/(ASCE)GT.1943-5606.0002699).

Graham, J., Alfaro, M., Ferris, G., 2004. Compression and strength of dense sand at high pressures and elevated temperatures. *Canadian Geotechnical Journal*, 41(6): 1206-1212.

Halliday, D., Resnick, R., Walker, J., 2014. *Fundamental of Physics*. 10th Edition, Wiley and Sons, New York. 1456pp.

Hausmann, M.R (1990). *Engineering Principles of Ground Modification*. McGraw-Hill, 632 pp.

Heravi, M., Cheshmi, A., 2023. Investigation of the effect of polymer emulsion on the uniaxial compressive strength of aeolian sand. *Civil Infrastructure Researches*, 9(1): 175-191.

Heravi, M., Cheshmi, A., 2024. Investigation impact of polymer emulsion on shear strength of aeolian sand. *Ferdowsi Civil Engineering*, 37(1-45): 111-126

Jefferson, I., 1994. Temperature effects on clay soils. Ph.D. thesis, Loughborough University.

Kazemi, R., Davoodi, M.H., 2012. Investigation on the effect of curing time on uniaxial strength of clayey soils strengthened by saturated lime solution. *World Applied Sciences Journal*, 19(11): 1607-1612.

Karner, S.L., Chester, J.S., Chester, F.M., Kronenberg, A.K., Hajash, A., 2005. Laboratory deformation of granular quartz sand: Implications for the burial of clastic rocks. *AAPG bulletin*, 89(5): 603-625.

Khan, H., 1982. Soil studies for highway construction in arid zones. *Engineering Geology*, 19(1): 47-62.

Khelifa, H., Ghrici, M., Kenai, S., 2010. Effect of curing time on shear strength of cohesive soils stabilized with combination of lime and natural pozzolan. *International Journal of Civil Engineering*, 9(2): 90-96.

Laloui, L., 2001. Thermo-mechanical behavior of soils. *Revue française de génie civil*, 5(6): 809-843.

Liu, H., Liu, H., Xiao, Y., McCartney, J.S., 2018. Effects of temperature on the shear strength of saturated sand. *Soils and Foundations*, 58(6): 1326-1338.</sup>

- Ma, Q., Shu, H., Xiao, H., Huang, C., 2020. Temperature-controlled triaxial compression test of tire strip-reinforced silty clay. *Arabian Journal for Science and Engineering*, 45: 4247-4256.
- Moayed, R.Z., Izadi, E., Heidari, S., 2012. Stabilization of saline silty sand using lime and micro silica. *Journal of Central South University*, 19 (10): 3006-3011.
- Mohammadi, F., Maghsoodi, S., Cheshomi, A., Rajabi, A.M., 2022. Unconfined compressive strength of clay soils at different temperatures: experimental and constitutive study. *Environmental Earth Sciences*, 81: 387. <https://doi.org/10.1007/s12665-022-10473-y>.
- Mohamedzein, Y., Al-Hashmi, A., Al-Abri, A., Al-Shereiqli, A., 2019. Polymers for stabilisation of Wahiba dune sands, Oman. *Proceedings of the Institution of Civil Engineers-Ground Improvement*, 172(2): 76-84.
- Neville, A.M., (2011). *Properties of Concrete*. Pearson Publications, Harlow. 846.pp.
- Osinubi, K.J., 1998. Permeability of lime-treated lateritic soil. *Journal of Transportation Engineering*, 124(5): 465-469.
- Padmakumar, G.P., Srinivas, K., Uday, K.V., Iyer, K.R., Pathak, P., Keshava, S.M., Singh, D.N., 2012. Characterization of aeolian sands from Indian desert. *Engineering Geology*, 139: 38-49.
- Punya-in, Y., Kongkitkul, W., 2023. Effects of temperature on the stress-strain-time behavior of sand under shear. *Journal of Testing and Evaluation*, 51(2): 686-705.
- Salih, N.B., Abdalla, T.A., 2023. Influence of curing temperature on shear strength and compressibility of swelling soil stabilized with hydrated lime. *Journal of Engineering Research*, 11(3): 2307-1877.
- Schotsmans, E.M., Denton, J., Dekeirsschieter, J., Ivaneanu, T., Leentjes, S., Janaway, R.C., Wilson, A.S., 2012. Effects of hydrated lime and quicklime on the decay of buried human remains using pig cadavers as human body analogues. *Forensic Science International*, 217(1-3): 50-59.
- Sherwood, P., 1993. *Soil stabilization with cement and lime*. HMSO, London. 153 pp.
- Shiva Kumar, M., Selvaraj, T., 2023. Ancient organic lime plaster production technology and its properties among Mayan, Egyptian, Persian and Asian civilizations. *Asian Journal of Civil Engineering*, 24(5): 2709-2718.
- Souza Júnior, P.L., Santos Junior, O.F., Fontoura, T.B., Freitas Neto, O. 2020. Drained and undrained behavior of an aeolian sand from Natal, Brazil. *Soils and Rocks*, 43(2): 263-270.
- Tai, P., Wang, X., Zhang, L. and Chen, R., 2024. Thermal effects on the shear behaviour of saturated coarse-grained soils with reference to post-earthquake deposits. *Acta Geophysica*, 72(4): 2223-2230.
- Wang, M., Benway, J.M., Arayssi, A.M., 1990. The effect of heating on engineering properties of clays. *ASTM Special Technical Publication*, 139-158.
- Wang, S., Huang, Y., 2022. Experimental study on the shear characteristics of quartz sand exposed to high temperatures. *Acta Geotechnica*, 17: 5031-5041.
- Zhang, Y., Daniels, J.L., Cetin, B., Baucom, I.K., 2020. Effect of temperature on pH, conductivity, and strength of lime-stabilized soil. *Journal of Materials in Civil Engineering*, 32(3). [https://doi.org/10.1061/\(ASCE\)MT.1943-5533.0003062](https://doi.org/10.1061/(ASCE)MT.1943-5533.0003062)
- Yavari, N., Tang, A.M., Pereira, J.M., Hassen, G., 2016. Effect of temperature on the shear strength of soils and the soil-structure interface. *Canadian Geotechnical Journal*, 53(7): 1186-1194.
- Yusof, Z., Zainorabidin, A., Osman Suliman, M.A., Omar Abu Osba, O.E., 2023. Effect of palm fiber-hydrated lime composition on the permeability of stabilised sandy soil. *International Journal of Sustainable Construction Engineering and Technology*, 14(2): 1-6.
- Yu, H., Chen, W., Gong, Z., Ma, Y., Chen, G., Li, X., 2018. Influence of temperature on the hydro-mechanical behavior of Boom Clay. *International Journal of Rock Mechanics and Mining Sciences*, 108: 189-197.
- Zhao, L., Tang, J., Zhou, M., Shen, K., 2022. A review of the coefficient of thermal expansion and thermal conductivity of graphite. *New Carbon Materials*, 37(3): 544-555

